International Journal of Mass Spectrometry 299 (2011) 151–157

Contents lists available at ScienceDirect

International Journal of Mass Spectrometry

journal homepage: www.elsevier.com/locate/ijms

Effects of higher-order multipoles on the performance of a two-plate quadrupole ion trap mass analyzer

Zhiping Zhang[a], Hannah Quist[b], Ying Peng[a], Brett J. Hansen[a,b], Junting Wang[a], Aaron R. Hawkins[b], Daniel E. Austin[a,*]

[a] Department of Chemistry and Biochemistry, Brigham Young University, C-310 BNSN, Provo, UT 84602, United States
[b] Department of Electrical and Computer Engineering, Brigham Young University, Provo, UT 84602, United States

ARTICLE INFO

Article history:
Received 4 August 2010
Received in revised form 12 October 2010
Accepted 16 October 2010
Available online 23 October 2010

Keywords:
Microfabricated ion trap mass spectrometer
Two-plate quadrupole ion trap
Planar ion trap
Octopole
Dodecapole
Higher-order multipole

ABSTRACT

We report on the effects of varying higher-order multipole components on the performance of a novel radiofrequency quadrupole ion-trap mass analyzer, named the planar Paul trap. The device consists of two parallel ceramic plates, the opposing surfaces of which are lithographically imprinted with 24 concentric metal rings. Using this device, the magnitude and sign of different multipole components, including octopole and dodecapole, can be independently adjusted through altering the voltages applied to each ring. This study presents a systematic investigation of the effects of the octopole and dodecapole field components on the mass resolution and signal intensity of the planar Paul trap. Also, the effect of dipole amplitude and scan speed under both forward and reverse scan modes have been investigated for various combinations of octopole and dodecapole. A trapping field in which the magnitudes of the octopole and dodecapole are, respectively, set to 0% and +8% of the magnitude of the quadrupole yields the highest mass resolution under the conditions studied. A small threshold voltage for dipole resonance ejection is observed for positive octopole, and to a lesser extent for positive dodecapole, but not for negative poles. When both octopole and dodecapole are negative, a reverse scan produces higher resolution, but this effect is not observed when only one of the components is negative.

1. Introduction

Over the past few decades ion trap mass spectrometers have found applications in a broad range of areas including physics [1], biology [2], environmental sciences [3], and many others [4,5]. In contrast to other types of mass analyzers (e.g., electric and magnetic sectors, time-of-flight), ion storage and confinement in an ion trap are accomplished using a time-dependent, radio-frequency (RF) electric field. By scanning the RF voltage or frequency, or by applying a supplemental ac signal, the trapped ions are ejected out of the confining electric field according to their different mass-to-charge ratios [6].

The mass resolution, sensitivity and mass measurement accuracy of an ion trap are strongly dependent on the contributions of higher-order components [7] in the trapping field. Although an ideal quadrupole ion trap contains only monopole and quadrupole potentials, all real electrode arrangements create higher-order multipole fields, such as octopole, dodecapole, etc. In commercial ion trap mass analyzers, performance is optimized by modifying the shape and/or arrangement of trap electrodes. For instance, the original Finnigan ion trap used additional space between electrodes, essentially "stretching" the trap by 10.8% in the axial (ejection) direction. This modification changed the higher-order field components, and allowed much better performance than the unstretched version [8]. Bruker–Franzen instruments use an ion trap with a modified hyperbolic angle geometry [9]. To maximize the quadrupole field component relative to the higher-order field components, Wells et al. [10] optimized the geometry of a cylindrical ion trap through field calculations using the Poisson/Superfish code and through experimental variation of the electrode structure. In each case, changing the geometric structure of the trap introduces or modifies higher-order components of the electric field in the trapping region [11]. Numerous studies have examined the effect on higher-order multipoles resulting from geometric factors such as the endcap holes or apertures [12–15], electrode alignment [12,16–18] and others [19].

Wu et al. studied the effects on the electric field of a cylindrical ion trap by changing its geometric structure [16]. Through geometric optimization, a "−10% compensation" criterion was suggested: the sum of octopole and dodecapole components should be −10% of the quadrupole component. By optimizing the geometry of the rectilinear ion trap, Ouyang et al. also found that when the

* Corresponding author. Tel.: +1 801 422 1551.
E-mail addresses: austin@chem.byu.edu, dea@byu.edu (D.E. Austin).

1387-3806/$ – see front matter © 2010 Elsevier B.V. All rights reserved.
doi:10.1016/j.ijms.2010.10.022

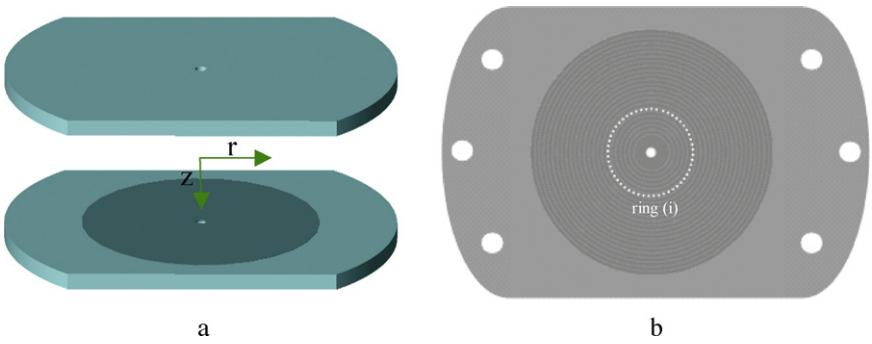

Fig. 1. Schematics of (a) the distribution of ring electrodes and (b) the trapping plates for the planar Paul trap.

sum of octopole and dodecapole components was about −10%, the trap demonstrated good performance [20]. However, Tallapragada et al. [12] regarded the "−10% compensation" rule as a compromise result. After geometry optimization of a cylindrical ion trap with the boundary element method (BEM), which possesses the same geometry as that of Wu et al. [16], they concluded that when the octopole and dodecapole components (namely, A_4/A_2 and A_6/A_2) were, respectively, 96.1% and 0.3%, the trap appeared good performance although A_4/A_2 is unusually large. Gill et al. investigated the effects of stretching and compressing the z_0 dimension of an ion trap via *in situ* optimization [21]. At the optimum stretch (∼9%), both signal intensity and resolution were improved while mass accuracy was maintained.

Several theoretical approaches have been employed to optimize the geometries of ion trap mass analyzers. All approaches include calculation of the multipole expansion of candidate trap geometries followed by optimization. The Cooks group has demonstrated this approach using a multi-particle trajectory simulation program, ITSIM [16,22,23]. After numerical computations of field composition, a few candidate geometries were manually selected using the "−10% compensation" criterion. Next, the ITSIM program was used to simulate the performance of the ion trap, and then experimental verification was carried out to identify the best geometry [16]. Another method, developed by Tallapragada et al. [12], minimized the difference between the calculated and the desired multipole components to reach optimum geometry [12,24]. SIMION 7.0 software [25] has also been used to determine the multipole expansion of a given electrode arrangement and geometry [18,26]. All of these approaches directly associate electrode geometry and field shape, and thus work within the constraints of electrode shape and position.

Although geometry change is the most common approach to optimize the electric field in the trapping region, odd-order multipole components (e.g., dipole and hexapole) can be modified by adding an ac signal, out of phase to each end cap, at the same frequency as the drive RF signal applied to the ring electrode. As reported by Splendore et al. [27], the addition of a "trapping field dipole" component to the normal "stretched" ion trap hyperbolic electrode geometry would generate both a dipole and a significant hexapole component in the trapping field. With such fields the detected ion signal intensity was doubled and the mass resolution was improved.

We have recently reported a new family of ion trap mass analyzers, including the Halo ion trap [28] and the planar Paul trap [29]. Different from conventional ion traps, such as cylindrical, rectilinear, linear, and toroidal ion traps, which utilize 3-dimensional metal electrodes to produce the appropriate electric fields, the trapping fields for our reported traps were realized by an array of metal electrode rings lithographically imprinted on ceramic disks [28–30]. The trapping fields in both traps were similar to those produced by machined metal electrodes. In contrast to traps made using 3-dimensional metal electrodes, the trapping fields in our devices can easily be adjusted by changing the voltages applied to different electrode rings, rather than by changing the geometries or positions of the electrodes. The contribution of each multipole component (e.g., octopolar field and dodecapolar field) to the trapping field can be independently adjusted by changing the voltage to each ring. These devices allow study of the effects of higher-order field components on mass analysis. The present study examines the effects of higher-order field components on the performance of the planar Paul trap. Because the lowest even-order terms above quadrupole (i.e., octopole, dodecapole) are expected to have a larger effect on ion behavior than much higher terms (i.e., above 16-pole), this study focuses on these lower terms.

2. Experimental

2.1. Optimization methodology

The device used in the present study consisted of an assembly of two plates (Fig. 1a). One surface of each plate was lithographically patterned with 24 metal rings, as illustrated in Fig. 1b. The dimensions of the device and locations of the rings were given previously [29]. Because the outer rings did not make a significant contribution to the electric potential at the trap center, only the first 11 rings were used in the present study. The outer 13 rings were electrically shorted to ring 11. The 1st and 24th rings were grounded in simulations, since the experimental setup was constrained by the design of the printed circuit boards (PCBs). The remaining rings were connected to capacitors in an RF capacitive voltage divider, located on PCBs behind each patterned plate. The primary drive RF was directly applied on the 24th ring, and the RF amplitude on each ring was determined by the choice of capacitor value associated with that ring.

SIMION and MATLAB were used to calculate the multipole expansion corresponding to each ring electrode, using an approach similar to our recent theoretical study [7]. Specifically, SIMION potential arrays were set up for each ring (with all other rings at zero). The potential was recorded at each grid unit along the z axis – perpendicular to the planar electrodes as shown in Fig. 1a. These potential values were imported into MATLAB and a least-squares fit of the nominally quadratic electric potential was calculated. Determination of the multipoles with the least-squares fit in MATLAB R2008b was performed as a polynomial with up to 20 poles to obtain the desired degree of accuracy for the lower order multipoles.

As recently demonstrated [7], the multipole components in the electric field of this type of trap can be approximately obtained by adding the multipole component contributions of each individual ring. By the superposition principle, the multipole expansion of the entire trap is the sum of the normalized multipole expansion

contributed by each individual ring electrode, weighted by the RF amplitude applied to that ring:

$$A_2 \approx \sum_{\text{ring}=2}^{\text{ring}=11-23} (V_{\text{ring}(i)} \cdot A_2)$$
$$A_4 \approx \sum_{\text{ring}=2}^{\text{ring}=11-23} (V_{\text{ring}(i)} \cdot A_4) \quad (1)$$
$$A_6 \approx \sum_{\text{ring}=2}^{\text{ring}=11-23} (V_{\text{ring}(i)} \cdot A_6)$$

where $V_{\text{ring}(i)}$ is the voltage applied to ring i; $A_{2,\text{ring}(i)}$, $A_{4,\text{ring}(i)}$, and $A_{6,\text{ring}(i)}$ are the normalized contributions of quadrupolar field, octopolar field, and dodecapolar field for ring i; and A_n is the multipole term for the entire device.

The RF amplitudes for each ring, and the corresponding capacitor values, were determined using the Solver function in Microsoft Excel. This method calculates the percentages of A_4/A_2 and A_6/A_2 if the voltages applied to different rings are known, and also calculates the voltages applied to different rings if the percentages of A_4/A_2 and A_6/A_2 are fixed.

The goals of the present study were two-fold: (1) to isolate and understand the effects of octopole and dodecapole components on the performance of the planar Paul trap, and (2) to determine combinations of fields that yield optimized performance. In order to isolate and understand the effects of the higher-order field components, a series of experiments were conducted in which one component was varied over a wide range while the other was held constant. Values of octopole and dodecapole components corresponding to the "−10% compensation rule" were also used for the sake of comparison. All other variables were held constant to the extent possible. Specifically, intermediate values of ion mass and scan speed were used. While these conditions do not yield the best possible mass resolution for this device, they establish a constant baseline from which to isolate and compare the effect of the higher-order multipoles. Following this comparison, spectra taken using "best" conditions are presented.

2.2. Experimental verification

The performance of the planar Paul trap with different electric fields was tested in an instrumental setup as described previously [29]. The setup includes an electron gun assembly, trapping region, and an electron multiplier detector. Behind each of the two ceramic plates comprising the trapping region was a PCB with a capacitor network. The capacitor network was used to establish the voltages on each of the ring electrodes under RF excitation. Spring-loaded pins were soldered to the PCBs in order to make electrical contact with the back sides of the trapping plates. A 6-mm stainless steel spacer was mounted between the trapping plates. Holes in the spacer admitted the electron beam, sample vapor, helium gas, and a Teflon tube leading to a Pirani gauge (Kurt J. Lesker, Clairton, CA). An RF signal with a frequency of 1.26 MHz and variable amplitude up to 738 $V_{0\text{-}p}$ (PSRF-100, Ardara Technologies, North Huntingdon, PA) was applied to the capacitor network on the PCBs, and the spacer was grounded. In addition, a supplementary low-voltage ac signal, generated using a 30 MHz synthesized function generator (DS345, Stanford Research Systems, Sunnyvale, CA) and a converter having two outputs with 180° phase difference, and amplified by a custom-made amplifier, was applied between the trapping plates to provide a dipole field for resonant ion ejection during the RF scan. The amplified supplementary ac signals were applied to the innermost ring on each plate, using a simple filter circuit to isolate the supplementary ac from the main RF signals. The applied frequency of the ac signal was 345 kHz, and β_z was approximately 0.55. The other operational details of the planar Paul ion trap are similar to those described in our recent study [29]. An electron multiplier detector (DeTech Detector Technology Inc., Palmer, MA) was used to detect the ejected ions, with a detector voltage operated at −1650 V. The signal was amplified (427 Current Amplifer, Keithley Instruments, Cleveland, OH) and recorded using a digital oscilloscope (WaveRunner 6000A, LeCroy, Chestnut Ridge, NY). Error bars in the data shown represent the observed standard deviation of several spectra taken under identical conditions, and do not represent factors such as electrode alignment that may change as PCBs are switched between experiments.

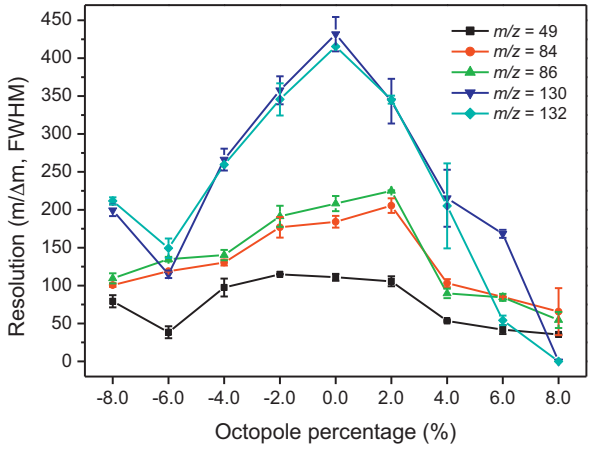

Fig. 2. Comparison of resolution ($m/\Delta m$, FWHM) for the m/z 49, 84, and 86 ions of dichloromethane, and the m/z 130 and 132 Th ions of trichloroethylene using different octopolar fields while keeping the dodecapole percentage at −4.0% under forward scan mode. These values are from individual spectra. Each data point represents the average of three measurements.

For all experiments, helium was used as the buffer gas at an indicated pressure of 5.34×10^{-3} Torr (uncorrected, 1 Torr = 133 Pa) as read from the Pirani gauge. Headspace vapor of the organic compounds of interest, without further purification, was leaked into the vacuum through two Swagelok leak valves (Swagelok, Solon, OH) to maintain a nominal pressure of $1.0\text{–}8.0 \times 10^{-5}$ Torr. *In situ* electron ionization was achieved using a custom-built electron gun comprising an iridium-filament, lens, gate, and a 1.6-amp power supply.

3. Results and discussion

3.1. Effect of octopole and dodecapole on the performance of the planar Paul trap

Fig. 2 shows the effect of the octopole component (A_4/A_2) on the mass resolution ($m/\Delta m$, FWHM) for the m/z 49, 84, and 86 ions of dichloromethane, and the m/z 130 and 132 ions of trichloroethylene. The dodecapole (A_6/A_2) was held constant at −4.0%. In general, mass resolution reaches a maximum at 0% octopole, dropping off for both positive and negative values. In addition, resolution is higher for heavier ions. In their optimization of cylindrical ion traps, Wells et al. also observed that when the octopole component (A_4/A_2) was close to 0.0%, the trap demonstrated a better performance [10], consistent with the present study.

It may be surprising that resolution does not drop off more quickly for negative values of octopole. Franzen et al. [31] showed that a negative octopole component in a conventional ion trap causes delayed ion ejection and reduced mass resolution, whereas a positive octopole has the opposite effect. Two important differ-

Table 1
The relative weights of octopole (A_4/A_2), dodecapole (A_6/A_2), hexadecapole (A_8/A_2), ikosipole (A_{10}/A_2), and tetraikosipole (A_{12}/A_2) used in each experiment shown in Fig. 2.

A_4/A_2 (%)	A_6/A_2 (%)	A_8/A_2 (%)	A_{10}/A_2 (%)	A_{12}/A_2 (%)
8.00	−4.00	−42.23	140.20	−312.51
6.00	−4.00	−40.59	136.81	−304.93
4.00	−4.00	−38.95	133.41	−297.34
2.00	−4.00	−37.12	129.87	−289.56
0.00	−4.00	−35.68	126.61	−282.14
−2.00	−4.00	−34.05	123.21	−274.53
−4.00	−4.00	−32.31	119.77	−267.18
−6.00	−4.00	−30.46	116.27	−260.00
−8.00	−4.00	−28.66	113.45	−254.91

ences between Franzen's work and the present effort are that (1) ions were ejected at the stability boundary in the former case, but at a lower q_z in the present case, and (2) higher-order components beyond dodecapole are small in a conventional quadrupole ion trap, and are larger in the planar Paul trap. In the present study, the relative values of hexadecapole (A_8/A_2), ikosipole (A_{10}/A_2), and tetraikosipole (A_{12}/A_2) are much larger than that of octopole (A_4/A_2), as shown in Table 1, and are due to the large edge effects introduced by the two-plate design [30]. Table 1 also shows that

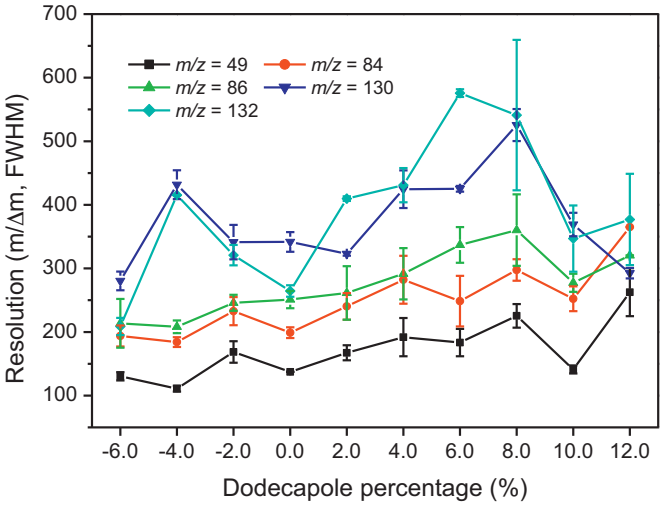

Fig. 3. Comparison of resolution ($m/\Delta m$, FWHM) for the m/z 49, 84, and 86 ions of dichloromethane, and the m/z 130 and 132 Th ions of trichloroethylene using different dodecapolar fields while keeping the octopole percentage at 0.0% under forward scan mode. These values are from individual spectra. Each data point represents the average of three measurements.

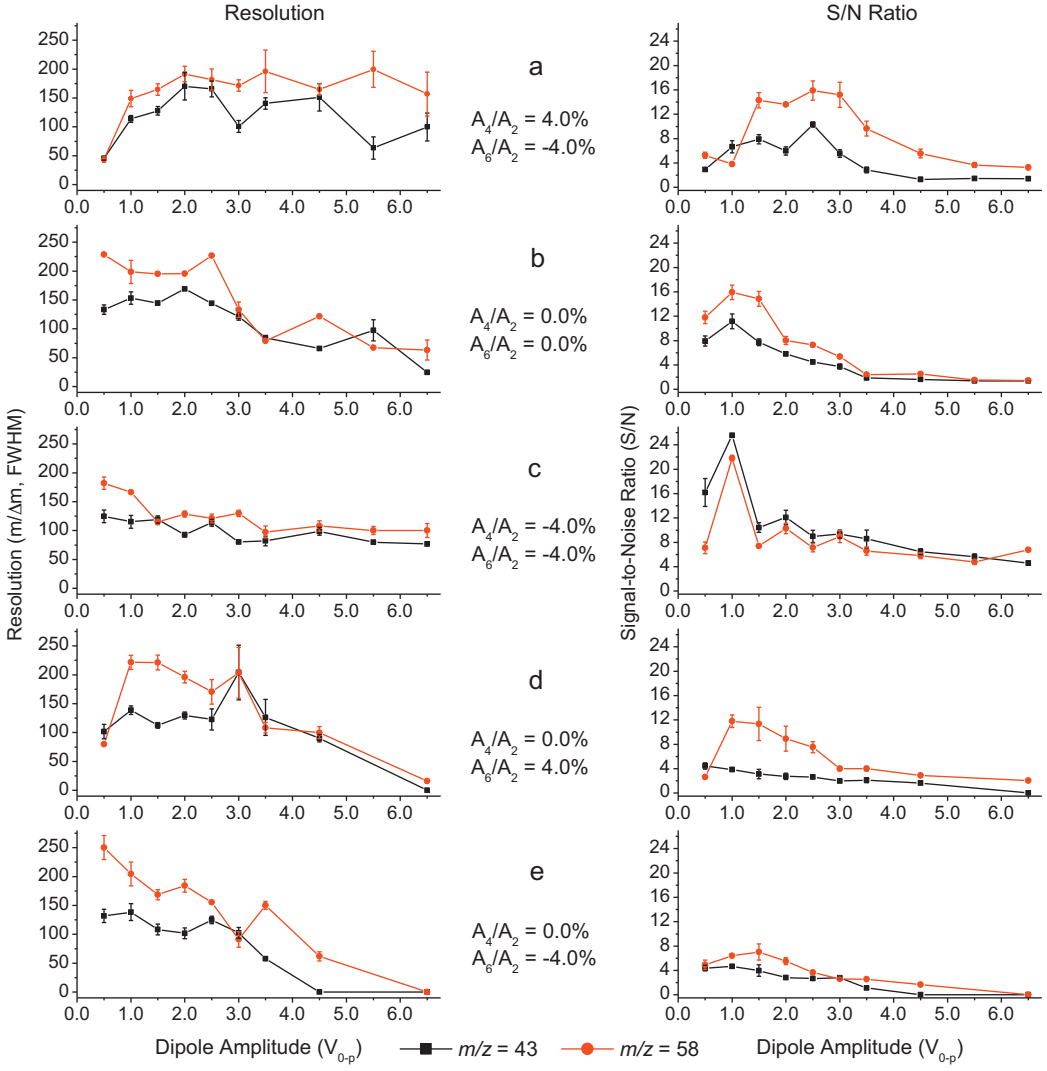

Fig. 4. Comparison of resolution ($m/\Delta m$, FWHM) and signal-to-noise (S/N) ratio for the m/z 43 and 58 ions of acetone using electric fields with different octopole/dodecapole combinations. These values are from individual spectra. Each data point represents the average of three measurements. Sample pressure: 10^{-5} Torr; ionization time: 4.0 ms; ac frequency: 345 kHz.

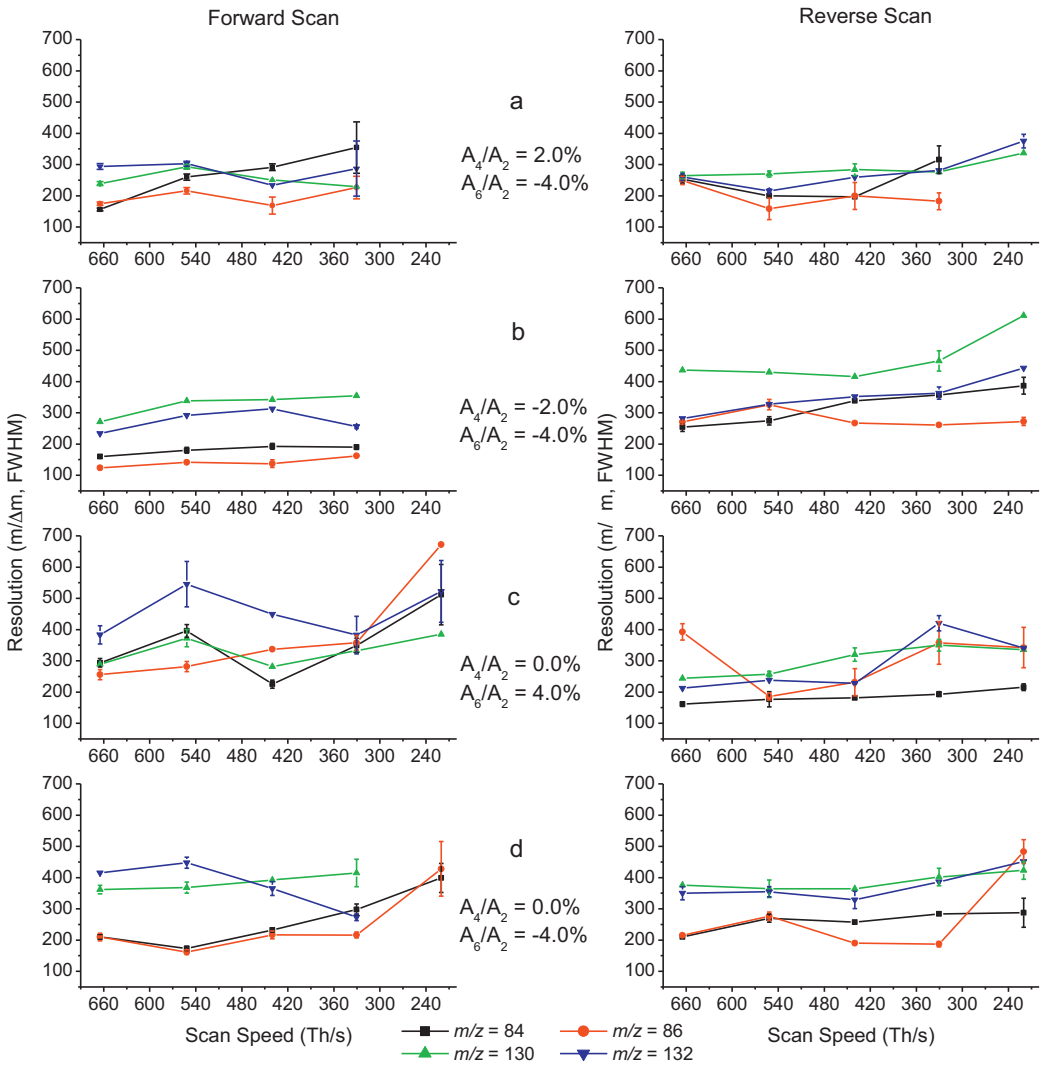

Fig. 5. Comparison of resolution ($m/\Delta m$, FWHM) for the m/z 84 and 86 ions of dichloromethane and the m/z 130 and 132 ions of trichloroethylene under the electric fields with different octopole/dodecapole combinations by using forward and reverse scan modes. These values are from individual spectra. Each data point represents the average of three measurements.

with the current design, as the octopole increases, holding dodecapole constant, the magnitude of the 16-, 20-, and 24-poles decreased. This variation in these higher-order poles may have had some effect on the results.

Fig. 3 shows mass resolution of these same peaks as the dodecapole (A_6/A_2) was varied. The octopole (A_4/A_2) was held constant at 0%. Highest mass resolution occurs when the dodecapole is in the range 8%. The effect of varying the dodecapole is not as dramatic as that of varying the octopole, demonstrating that the octopole has a greater effect on the ion ejection process.

3.2. Effect of dipole amplitude on resolution and S/N

Simulations reported by Franzen indicated that a higher dipole field is required to resonantly eject ions from a trap with a small positive octopole than from a trap with a pure quadrupole field [31]. In fact, when an octopole is present, a threshold voltage exists, below which ions cannot be resonantly ejected. We tested this result by varying the magnitude of the dipole field under different octopole/dodecapole combinations, and observing both the resulting mass resolution and the signal-to-noise ratio (S/N). The S/N ratio is indicative of the combined trapping and ejection efficiencies, assuming that the noise is fairly constant.

Fig. 4 shows the results of this experiment using five octopole/dodecapole combinations. In the case of a positive octopole (Fig. 4a) both S/N and resolution drop off significantly for the lowest dipole amplitudes. A similar trend is observed, although not as strongly, for a positive dodecapole (Fig. 4d). For the other field combinations (Fig. 4b, c, and e) the highest resolution is achieved using the smallest amplitude of applied dipole, and S/N does not appear to drop off significantly at the lowest dipole amplitudes. Unfortunately, the trend is not well defined from these data. Nevertheless, these results are in general agreement with Franzen et al. [31]. In all cases, both resolution and S/N decrease with higher dipole amplitude, although with 4% octopole the dipole amplitude must be higher than in the other cases for this trend to appear. Except at the minimum applied dipole signal, the dodecapole appears to have little effect on the resolution or S/N.

3.3. Effect of scan speed and scan direction on mass resolution and signal

Generally, mass resolution in an ion trap increases with decreasing RF scan speed [32–35]. The effect of scan speed on the performance of the planar Paul trap was investigated within the range of 665–220 Th/s. Fig. 5 shows mass resolution as a function

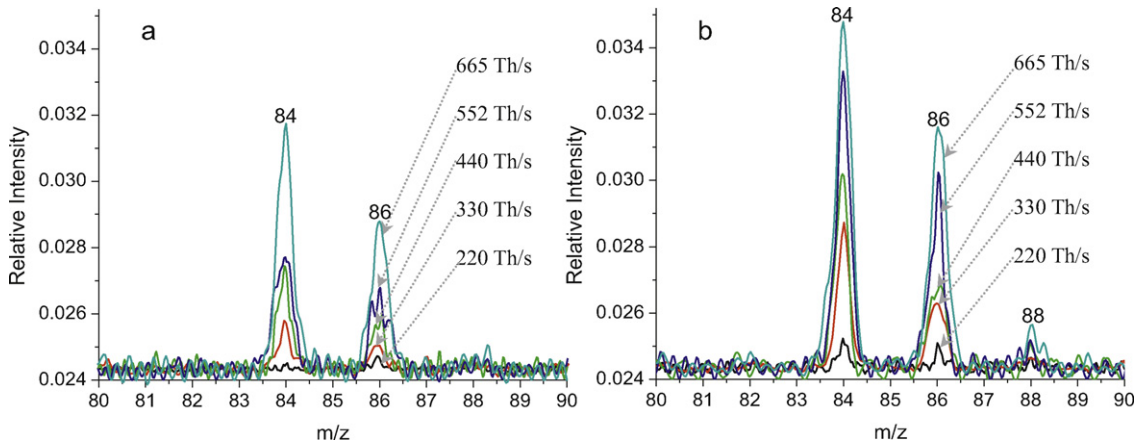

Fig. 6. Comparison of peak intensity for the *m/z* 84 and 86 ions of dichloromethane using the electric field with 0.0% octopole and −4.0% dodecapole components. Both forward (a) and reverse scan modes (b) are shown.

of scan speed for several octopole/dodecapole configurations. Ions used include the *m/z* 84 and 86 fragments of dichloromethane and the *m/z* 130 and 132 of trichloroethylene. Both forward and reverse scan modes were carried out for each speed and each field. Little difference was observed in forward scans between +2 and −2% octopole, holding the dodecapole constant at −4%, consistent with the data shown in Fig. 2. However, with reverse scan, the negative octopole had a notably higher resolution than the positive octopole, and higher than the forward scan with the same field. With the octopole fixed at 0% and the dodecapole varied from −4% to +4% no significant difference existed between forward and reverse scans, or between positive and negative dodecapole. Resolution increased slightly with reduced scan speed for all field combinations.

Several previous studies have compared mass resolution between forward and reverse scans in conventional ion traps [36–39]. These investigations indicated that the resolution obtained using the reverse scan depended on the octopole contribution in the trapping field. For the stretched geometry, with a positive octopole component, mass resolution in a forward scan was much better than that in a reverse scan [36–38]. Conversely, a compressed trap with a negative octopole term demonstrated better resolution in the reverse scan than that in the forward scan [38,40]. Williams et al. [36] attributed this observation to an effect analogous to Doppler focusing or defocusing, dependent on scan direction relative to the direction of the ion frequency shift with oscillatory amplitude. In a field with positive octopole – that is, the octopole has the same sign as the quadrupole along the axis of ion ejection – the secular frequency of ions increases with increasing amplitude of secular motion. In a field with negative octopole, the secular frequency of an ion decreases with the amplitude of motion. As the RF amplitude is ramped upward (forward scan), the secular frequency of a given ion increases until it nearly coincides with the frequency of the applied dipole signal. At this point the ion becomes resonantly excited, and the amplitude of its secular motion increases. A positive octopole will cause the frequency of

Table 2
Comparison of signal-to-noise ratio for the *m/z* 130 peak of trichloroethylene obtained using different values of the octopole component. Scan speed: 665 Th/s. Each data point represents the average of three measurements.

A_4/A_2 (%)	A_6/A_2 (%)	Forward scan	Reverse scan
2.00	−4.00	11.30 ± 0.85	89.28 ± 9.18
−2.00	−4.00	19.45 ± 1.53	16.72 ± 0.07
0.00	4.00	14.15 ± 0.91	30.36 ± 5.89
0.00	−4.00	16.16 ± 1.15	21.40 ± 1.31

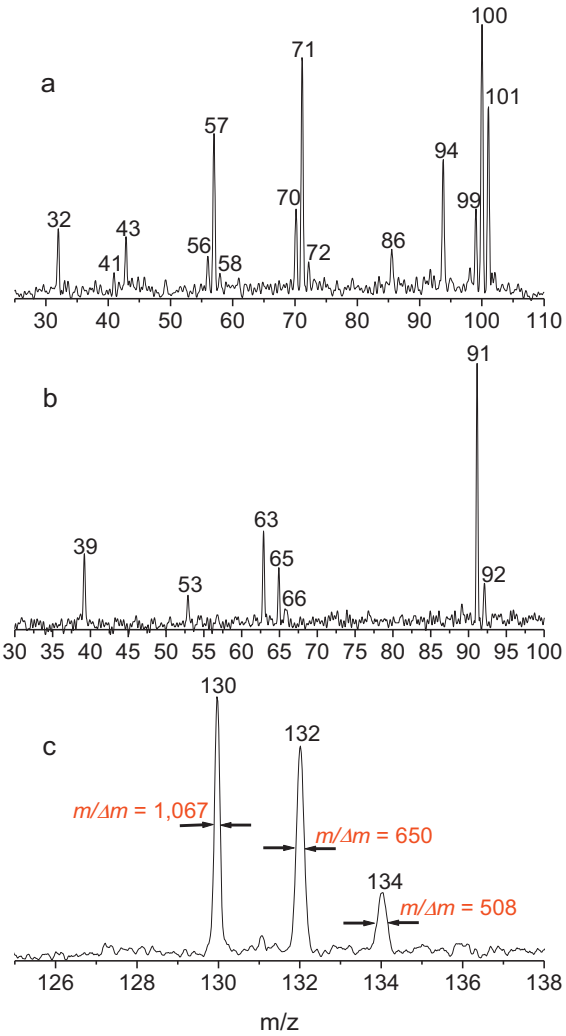

Fig. 7. Mass spectra of (a) heptane, (b) toluene and (c) trichloroethylene using 2.14% octopole and 10.49% dodecapole components. Other conditions: (a) ionization time: 10 ms, scan speed: 330 Th/s, ac frequency: 345 kHz, scan mode: forward scan; (b) ionization time: 10 ms, scan speed: 110 Th/s, ac frequency: 340 kHz; scan mode: forward scan; and (c): ionization time: 4 ms, scan speed: 110 Th/s, ac frequency: 340 kHz, scan mode: reverse scan, and ac amplitude (1.4 $V_{0\text{-}p}$) is same for all the cases.

secular motion to increase further, drawing it closer to the applied signal and causing rapid ejection. Conversely, a negative octopole will pull the secular frequency away from the applied dipole frequency, delaying ejection. During a reverse scan, the opposite occurs, and a negative octopole causes rapid ejection and better resolution. Ding et al. [41] have reported a similar effect for forward and reverse scans using a digital ion trap. Rajanbabu et al. [42] suggested an alternative explanation in which the resolution in the forward and reverse scans in stretched Paul traps is attributable to the constraints on the pre-ejection initial conditions that ions possess. Coherence of ion motion in the forward scan and the absence of coherence in the reverse scan resulted in the observation of differing resolutions in the two directions. The experimental results in the present study are in general agreement with those from these previous studies.

The signal-to-noise (S/N) ratio for each experiment in Fig. 5 typically decreased as the scan speed was reduced, as illustrated in Fig. 6, consistent with previous results [32,43]. For extremely slow scans many peaks dropped below the noise. Table 2 shows the S/N at 665 Th/s for the m/z 130 ion for each field configuration and scan direction. For most octopole/dodecapole combinations, S/N was higher for the reverse scan. It is not clear why the {2% octopole, −4% dodecapole} combination has such a high S/N.

One of the goals of the present work was to identify the optimum electric field and scan conditions for the planar Paul trap. Fig. 7 shows mass spectra of three compounds taken using the most favorable operating conditions, as indicated. Important fragment peaks for each compound are identified. Fig. 6c shows the effect of space-charge on mass resolution for the closely spaced isotope peaks of trichloroethylene. The higher-mass ions are scanned out first, and experience space-charge from the adjacent peaks during ejection. The ions at m/z 130 are ejected without this effect, resulting in the highest mass resolution (>1000) of the three.

4. Conclusions

The optimization of electric fields in a planar Paul trap can be easily achieved by manipulating the voltages applied to discrete, patterned electrode rings. For this approach, the contribution of the multipole components (e.g., quadrupole, octopole, dodecapole, and so on) from different electrodes was first obtained through the ion optical simulation program SIMION and an equation solver. Target voltages were obtained by constructing a capacitor network on a printed circuit board and connecting it to plates containing the trap's ring electrodes. Experimental demonstrations of the effects of octopole and dodecapole components on the performance of the planar Paul trap have been presented and suggest that significant improvements to resolution and signal-to-noise ratio can be obtained by adjusting the multipole components in the trapping potential. It is believed that a similar optimization procedure can be extended to the electric fields of other ion traps, such as the Halo trap [28] and others being developed by our research group.

Acknowledgments

This work was supported by the NASA Planetary Instrument Definition and Development Program, NNH06ZDA001N. We also gratefully acknowledge many helpful discussions with Dr. Wei Xu at Purdue University on calculations of multipole components.

References

[1] R. Maiwald, D. Leibfried, J. Britton, J.C. Bergquist, G. Leuchs, D.J. Wineland, Nat. Phys. 5 (2009) 551.
[2] H.Y. Wu, V.S.M. Tseng, L.C. Chen, Y.C. Chang, P.P. Ping, C.C. Liao, Y.G. Tsay, J.S. Yu, P.C. Liao, Anal. Chem. 81 (2009) 7778.
[3] M. Gros, M. Petrovic, D. Barcelo, Anal. Chem. 81 (2009) 898.
[4] H. Hiura, T. Kanayama, J. Mol. Struct. 735 (2005) 367.
[5] C. Wold, R. van de Grampel, Polym. Test. 28 (2009) 495.
[6] G.C. Stafford Jr., P.E. Kelley, J.E.P. Syka, W.E. Reynolds, J.F.J. Todd, Int. J. Mass Spectrom. 60 (1984) 85.
[7] D.E. Austin, B.J. Hansen, Y. Peng, Z. Zhang, Int. J. Mass Spectrom. 295 (2010) 153.
[8] J.E.P. Syka, in: R.E. March, J.F.J. Todd (Eds.), Practical Aspects of Ion Trap Mass Spectrometry, vol. 1, CRC Press, New York, USA, 1995, p. 169.
[9] M. Sudakov, Int. J. Mass Spectrom. 206 (2001) 27.
[10] J.M. Wells, E.R. Badman, R.G. Cooks, Anal. Chem. 70 (1998) 438.
[11] R.E. March, F.A. Londry, R.L. Alfred, Org. Mass Spectrom. 27 (1992) 1151.
[12] P.K. Tallapragada, A.K. Mohanty, A. Chatterjee, A.G. Menon, Int. J. Mass Spectrom. 264 (2007) 38.
[13] H. Koizumi, W.B. Whitten, P.T.A. Reilly, E. Koizumi, Int. J. Mass Spectrom. 281 (2009) 108.
[14] M. Chattopadhyay, N.K. Verma, A.K. Mohanty, Int. J. Mass Spectrom. 282 (2009) 112.
[15] M. Chattopadhyay, A.K. Mohanty, Int. J. Mass Spectrom. 288 (2009) 58.
[16] G. Wu, R.G. Cooks, Z. Ouyang, Int. J. Mass Spectrom. 241 (2005) 119.
[17] M.G. Blain, L.S. Riter, D. Cruz, D.E. Austin, G. Wu, W.R. Plass, R.G. Cooks, Int. J. Mass Spectrom. 236 (2004) 91.
[18] A. Chaudhary, F.H.W. van Amerom, R.T. Short, S. Bhansali, Int. J. Mass Spectrom. 251 (2006) 32.
[19] A.N. Konenkov, D.J. Douglas, N.V. Konenkov, Int. J. Mass Spectrom. 289 (2010) 144.
[20] Z. Ouyang, G. Wu, Y. Song, H. Li, W.R. Plass, R.G. Cooks, Anal. Chem. 76 (2004) 4595.
[21] L.A. Gill, J.W. Amy, W.E. Vaughn, R.G. Cooks, Int. J. Mass Spectrom. 188 (1999) 87.
[22] H.A. Bui, R.G. Cooks, J. Mass Spectrom. 33 (1998) 297.
[23] W.R. Plass, Ph.D. Thesis, Justus-Liebig-Universität Gießen, Germany (2001).
[24] A. Krishnaveni, N.K. Verma, A.G. Menon, A.K. Mohanty, Int. J. Mass Spectrom. 275 (2008) 11.
[25] D.A. Dahl, Int. J. Mass Spectrom. 200 (2000) 3.
[26] F.H.W. van Amerom, A. Chaudhary, M. Cardenas, J. Bumgarner, R.T. Short, Chem. Eng. Commun. 195 (2008) 98.
[27] M. Splendore, E. Marquette, J. Oppenheimer, C. Huston, G. Wells, Int. J. Mass Spectrom. 190/191 (1999) 129.
[28] D.E. Austin, M. Wang, S.E. Tolley, J.D. Maas, A.R. Hawkins, A.L. Rockwood, H.D. Tolley, E.D. Lee, M.L. Lee, Anal. Chem. 79 (2007) 2927.
[29] Z. Zhang, Y. Peng, B.J. Hansen, I.W. Miller, M. Wang, M.L. Lee, A.R. Hawkins, D.E. Austin, Anal. Chem. 81 (2009) 5241.
[30] D.E. Austin, Y. Peng, B.J. Hansen, I.W. Miller, A.L. Rockwood, A.R. Hawkins, S.E. Tolley, J. Am. Soc. Mass Spectrom. 19 (2008) 1435.
[31] J. Franzen, R.-H. Gabling, M. Schubert, Y. Wang, in: R.E. March, J.F.J. Todd (Eds.), Practical Aspects of Ion Trap Mass Spectrometry, vol. 1, CRC Press, New York, USA, 1995, p. 49.
[32] J.C. Schwartz, J.E.P. Syka, I. Jardine, J. Am. Soc. Mass Spectrom. 2 (1991) 198.
[33] D.E. Goeringer, S.A. McLuckey, G.L. Glish, Proc. 39th ASMS Conf. Mass Spectrometry and Allied Topics, Nashville, TN, 1991, p. 532.
[34] J.D. Williams, K. Cox, K.L. Morand, R.G. Cooks, R.K. Julian Jr., R.E. Kaiser, Proc. 39th ASMS Conf. Mass Spectrometry and Allied Topics, Nashville, TN, 1991, p. 1481.
[35] R.E. Kaiser, R.G. Cooks, G.C. Stafford, J.E.P. Syka, P.H. Hemberger, Int. J. Mass Spectrom. Ion Process. 106 (1991) 79.
[36] J.D. Williams, K.A. Cox, R.G. Cooks, S.A. McLuckey, K.J. Hart, D.E. Goeringer, Anal. Chem. 66 (1994) 725.
[37] G. Dobson, J. Murrell, D. Despeyroux, F. Wind, J.-C. Tabet, Rapid Commun. Mass Spectrom. 17 (2003) 1657.
[38] M. Wang, Proc. 43rd ASMS Conf. Mass Spectrometry and Allied Topics, Atlanta, GE, 1995, p. 1121.
[39] V.M. Doroshenko, R.J. Cotter, J. Am. Soc. Mass Spectrom. 8 (1997), 1141. J. M.
[40] Wells, W.R. Plass, R.G. Cooks, Anal. Chem. 72 (2000) 2677.
[41] L. Ding, M. Sudakov, F.L. Brancia, R. Giles, S. Kumashiro, J. Mass Spectrom. 39 (2004) 471.
[42] N. Rajanbabu, A. Chatterjee, A.G. Menon, Int. J. Mass Spectrom. 261 (2007) 159.
[43] S.A. McLuckey, G.J. van Berkel, G.L. Glish, J.C. Schwartz, in: R.E. March, J.F.J. Todd (Eds.), Practical Aspects of Ion Trap Mass Spectrometry, vol. 2, CRC Press, New York, USA, 1995, p. 89.